TABLE I

FERRITE DIGITAL PHASE SHIFTER PHASE SHIFT, LOSS AND POWER TRADEOFFS**

Band	P_p(kW)	P_{av}(W)	$4\pi M_s$	$\Delta\phi$/inch	LP 360°	Notes
X*	1	1	1800	150	0.35	1
X*	150	1	900	60	0.70	1
X*	50	400	1000	60	0.9	2, 4
C*	1	1	1800	100	0.40	1
C*	400	1	640	40	0.80	1
C*	50	500	825	38	0.65	2, 3
C	300	700	650	30	1.00	2, 4
S*	1	1	900	60	0.50	1
S	500	1	335	23	0.95	1
S*	100	900	425	26	0.8	2, 4
S	500	1000	350	20	1.00	2, 4

* Actual measured results.

** $\Delta\phi$/inch values shown are for low-power room temperature. LP 360° values shown are for operational devices at indicated power levels.

1. Al-doped YIG.
2. Gd-Al-doped YIG.
3. Water cooled with boron nitride cooling slabs.
4. Water cooled with boron nitride thermal conducting T sections.

CONCLUSION

Table I summarizes the type of ferrite phase shifter performance to be expected. Tradeoffs necessary to achieve high peak and average power levels are indicated. In designing for high peak and low average power levels, the saturation magnetization is normally reduced with only a small sacrifice in terms of loss, but a notable decrease in differential phase shift per inch. When high average power levels must also be handled, the use of gadolinium doping to improve $4\pi M_s$ stability and modification of the phaser structure to improve heat transfer both result in significant increase in loss per 360 degrees of differential phase shift. Some of these tabulated data represent results already achieved; some are predicted performance levels based on the computer-aided solution as supported by experimental results.

REFERENCES

[1] J. L. Allen, "The analysis of ferrite phase shifters including the effects of losses," Ph.D. dissertation, Georgia Institute of Technology, Atlanta, May 1966.

[2] B. Lax, K. J. Button, and L. M. Roth, "Ferrite phase shifters in rectangular waveguide," *J. Appl. Phys.*, vol. 25, p. 1413, 1954.

[3] W. J. Ince and E. Stern, "Computer analysis of ferrite digital phase shifters," *IEEE Internat'l Conv. Rec.*, vol. 14, pt. 5, pp. 32–38, 1966.

[4] E. Schlömann, "Theoretical analysis of twin-slab phase shifters in rectangular waveguide," *IEEE Trans. Microwave Theory and Techniques*, vol. MTT-14, pp. 15–23, January 1966.

[5] G. T. Rado, "On the electromagnetic characterization of ferrimagnetic media: permeability tensors and spin wave equations," *IRE Trans. Antennas and Propagation*, vol. AP-4, pp. 512–525, July 1956.

[6] D. Polder and J. Smit, "Resonance phenomena in ferrites," *Rev. Modern Phys.*, vol. 25, p. 89, 1953.

[7] S. Ramo and J. R. Whinnery, *Fields and Waves in Modern Radio*, 2nd ed. New York: Wiley, 1953, p. 353.

Lumped Elements in Microwave Integrated Circuits

DANIEL A. DALY, STANLEY P. KNIGHT, MARTIN CAULTON, SENIOR MEMBER, IEEE, AND ROALD EKHOLDT, MEMBER, IEEE

Abstract—**The use of lumped rather than distributed elements affords a considerable size reduction (typically a factor of 10 in area) in *L*- and *S*-band microwave integrated circuits. The electrical performance of such lumped elements is shown to be good enough to warrant their use in many applications where the size advantage or the resultant cost advantage is important. Miniature elements have been constructed which behave as true lumped reactive components up to at least 2.5 GHz. These elements have been evaluated using an impedance measurement method. Both inductors and capacitors have exhibited *Q*s greater than 50 at lower *S* band. Single-stage transistor power amplifiers at 2 GHz have been breadboarded using a simple arrangement of the lumped elements to match the measured impedances of the transistor pellet. These amplifiers have had gains as high as 4.7 dB at 2 GHz. The transistor used typically exhibits about 5 dB of gain in conventional coaxial circuitry. The loss in the lumped element matching networks has been about 0.5 dB greater than the loss in the distributed matching networks used in a microstrip amplifier built with the same type transistor. It is expected that the lumped circuit loss can be reduced as improved components are developed.**

Manuscript received June 12, 1967; revised August 30, 1967.

D. A. Daly and M. Caulton are with the RCA Laboratories, David Sarnoff Research Center, Princeton, N. J. 08540.

S. P. Knight was on temporary assignment to RCA Laboratories, David Sarnoff Research Center from RCA Astro-Electronics Division, Hightstown, N. J.

R. Ekholdt was on leave of absence to RCA Laboratories, David Sarnoff Research Center. He is with the Norwegian Defense Research Establishment, Kjeller, Norway.

I. INTRODUCTION

IT HAS BEEN well established that microwave integrated circuits will play an important role in future systems. Integrated switches,[1] amplifiers,[2] mixers,[3] and

oscillators[4] that operate at microwave frequencies have been described. These circuits have all used transmission lines as resonant elements. This paper will describe the use of minute lumped elements for microwave integrated circuits operating in S band.[1] It is important to note that true lumped microwave elements could not have been made without incorporating the advanced technology used for the fabrication of transistors and lower frequency integrated circuits. The lumped elements, because of performance limitations, cannot replace transmission lines in all S-band applications but they do have important uses for certain areas, and indeed an operating power amplifier is described in this paper.

The cost of an integrated circuit is roughly inversely proportional to the number of circuits processed simultaneously on a single starting wafer (ceramic or semiconductor). A fairly large number of X-band circuits using $\lambda/4$ transmission lines ($\lambda/4 \approx 0.125$ inch on Al_2O_3 substrate) can fit on a standard 1 by 1 inch wafer. Few S-band circuits, however, can fit on such a wafer. Thus, if many low-cost S-band circuits are to be made simultaneously, it is necessary to resort to lumped elements.[2]

Section II of this paper will briefly consider the quality characteristic Q of lumped elements. In Section III, the measurement techniques used to determine the impedance and Qs of lumped inductors and capacitors will be described. The results of these measurements on individual elements are described in Sections IV and V. In Section VI the feasibility of constructing amplifiers using elements wire bounded together is demonstrated. This is not an integrated circuit; however, some preliminary work on hybrid integrated amplifiers is reported. Finally applications of these elements in integrated circuits are suggested.

II. Considerations of Reactive Elements

The use of lumped elements in microwave integrated circuits has been considered by several workers,[5]–[8] but to our knowledge operating high-Q tuned circuits composed entirely of thin-film truly lumped components have not been reported at frequencies as high as S band. Fig. 1(a) schematically depicts a simple planar spiral inductor. The current in the inductor, to a first approximation, flows within a skin depth on the top and bottom surfaces and the inner vertical face of the inside turn and the outer vertical face of the outside turn. Fig. 1(a) ignores current crowding that occurs at the higher frequencies, and also leakage flux. The Q is the reactance X divided by the resistance R

$$Q = \frac{\omega L}{R} \tag{1}$$

where ω is the angular frequency and L is the inductance. A simple expression for Q can be derived by relating the resistance to the length and width of the spiral.

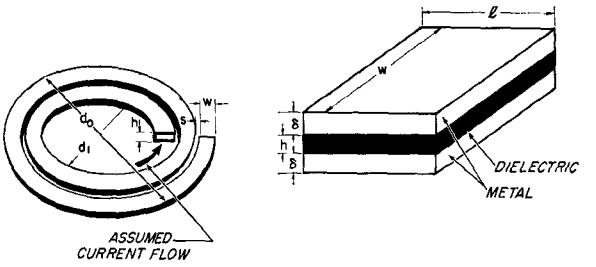

(a) (b)

Fig. 1. Sketch of reactive elements.

The ac resistance, ignoring the side walls and losses in the supporting substrate, is

$$R = \frac{an\pi R_s}{W} \tag{2}$$

where

$a = (d_0 + d_i)/4$ [average radius Fig. 1(a)]
n is the number of turns
R_s = surface resistivity in ohms per square $= \sqrt{\pi f \mu/\sigma}$
f is the frequency
μ is the permeability
σ is the conductivity.

Thus,

$$Q = \frac{2fLW}{R_s na} = \frac{2LW}{na}\sqrt{\frac{f\sigma}{\pi\mu}}. \tag{3}$$

According to (3), Q increases with the square root of the frequency. It is apparent that Q benefits by increasing W; keeping the inductance and average radius nearly constant. The maximum width W is limited by self resonance of the inductor resulting from parasitic interturn capacitance. Increasing W, however, would increase the coil size, defeating the purpose of using lumped elements. Inductors with Qs greater than 50 at 2 GHz with a diameter less than 0.050 inch will be reported in Section IV. Based on the assumed current flow, one needs coil heights h of the order of several skin depths; about 6 microns for copper or 8 microns for aluminum at 2 GHz. As the Q is proportional to the volume to surface ratio, circular spirals will have higher Qs than square ones.

Capacitors are now considered. Fig. 1(b) illustrates a simple metal-oxide sandwich capacitor. The metal thickness is 1 to 2 skin depths, about 2 to 4 microns at 2 GHz. A dielectric thickness of 0.5 to 1.0 micron for silicon dioxide appears practical. The loss behavior of a capacitor can be calculated using standard transmission line theory[9] and considering the capacitor to be a short length of open circuited transmission line. The capacitor Q_{cap} is found to be,

$$\frac{1}{Q_{\text{cap}}} = \frac{1}{Q_c} + \frac{1}{Q_d} \tag{4}$$

where the conductor Q_c (for a capacitance C of square area) is

$$Q_c \approx \frac{3}{2\omega R_s C} \propto f^{-3/2} \tag{5}$$

[1] The octave frequency band designation is used in this paper, i.e., L band = 1.0 to 2.0 GHz, S band = 2.0 to 4.0 GHz, C band = 4.0 to 8.0 GHz, and X band = 8.0 to 12.0 GHz.

[2] Another method of reducing size is to use transmission lines on high-dielectric constant substrates. These are in the early stages of development. There are problems that are yet to be solved.

and the dielectric Q_d is

$$Q_d \approx \frac{1}{\tan \delta} \tag{6}$$

where $\tan \delta$ is the loss tangent of the dielectric. At 2 GHz, the Q_c for most metals is greater than 500, and for fused quartz (SiO_2) $Q_d = 10\,000$. Unfortunately the values achieved in practice are orders of magnitude below the calculated value, as described in Section V.

III. Measurement Technique

The small size of lumped elements at microwave frequencies complicates their electrical evaluation. The properties of the elements can, however, be completely determined by slotted line impedance measurements, and this was the method used. The measurement system is illustrated in Figs. 2 and 3. The test component, an inductor in Fig. 3, terminates a 50 ohm microstrip line which is clipped onto an OSM connector. This fixture is connected through an adapter to a General Radio-900 precision slotted line. Measurements of VSWR and position of minimum are made and subsequently repeated with the test component replaced by a known termination; a short or an open circuit. The reactance and quality factor Q of the test component are determined by a comparison of the data for the three cases. Although the accuracy of the Q measurement is somewhat limited at the upper edge of the frequency band, this method has been selected for use because it yields both the reactance and Q of the test component over a range of frequencies in a direct manner.

In order to evaluate high-Q reactive components by this method, the transmission line between the slotted line and the test component should meet three requirements:

1) It should be well matched.
2) Its loss should be small compared to the loss in the test component.
3) The reactive end effect at the terminal point on the transmission line where the test component is attached should be negligible.

The system used in Fig. 2 exhibits the following behavior across the frequency band 0.5 to 2.5 GHz. The microstrip transmission line and adaptors terminated in a matched load have a VSWR of less than 1.05 over the frequency range. The VSWR measured on the system of Fig. 2 with open and short terminations is generally high, frequently greater than 200. The measured positions of minimum with open and short terminations are separated by one-quarter wavelength. Thus, all three requirements are fairly well satisfied. The fact that conditions 1) and 2) are not completely met leads to inaccuracies in the Q measurement which are discussed in the Appendix.

Microstrip transmission line is used in the test fixture because connecting joints between the test piece and the line are accessible with the test piece mounted at the end of the line. Mounting the test piece at the end of the 50 ohm line simplifies interpretation of the data. The 50 ohm microstrip line used has physical dimensions which are compatible both with the test pieces and with the OSM connector. The

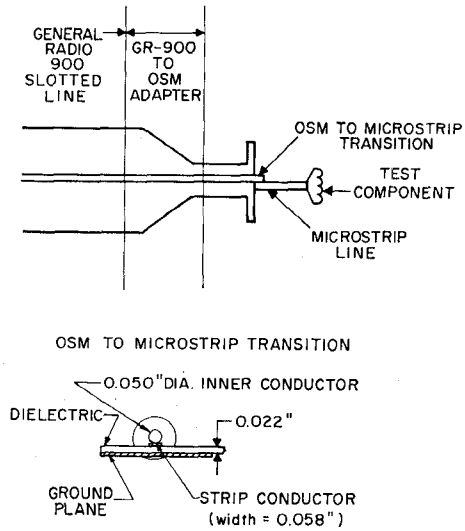

Fig. 2. Sketch of measurement system.

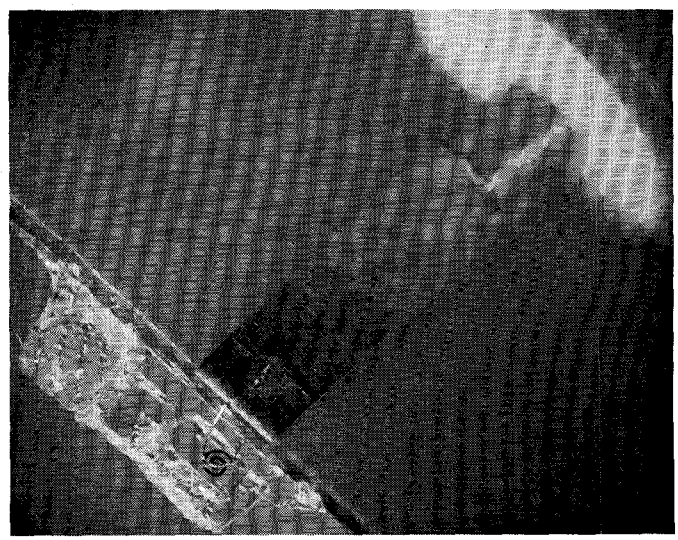

Fig. 3. Photograph of test fixture.

distance between the strip conductor and the ground plane is sufficiently small (0.022 inch) to make the end effect negligible.

The reactance of the test component is determined from the shift in the position of the minimum. Data are taken with the line terminated in several ways:

1) Terminated in a shorted component (shorted by a short wire connecting the ends of the element as shown in Fig. 3).
2) Terminated in the component (shorting wire removed).
3) Terminated in an open circuit (component removed).
4) Terminated in a short (tab of metal).

The lead reactance is determined from measurements 1) and 3) or 4). The total reactance of the leads plus the test component is found from measurements 2) and 3) or 4). Thus, the net reactance of the test component is determined. The accuracy of the reactance measurements has been very good. As an example, the lead inductance of a particular capacitor was determined from sets 1 and 3 to be 1.30 nH and from sets 2 and 3 to be 1.31 nH. Both determinations were made over the frequency range 0.5 to 2.5 GHz.

Component Q is evaluated from the VSWR data once the normalized reactance x is known. When a transmission line is terminated in a reactance and the VSWR is high (above 5 is sufficient), the VSWR is approximately

$$\text{VSWR} \approx |x| Q + \frac{Q}{|x|} + \frac{|x|}{Q}.$$

This expression is derived by combining the following transmission-line relationships, expressed here in functional form: reflection coefficient $\rho = f(\text{normalized impedance}) = f(|x|, Q)$ and $|\rho| = f(\text{VSWR})$. For the components under consideration the last term $|x|/Q$ on the right-hand side is negligible. Since very high VSWRs are measured, the double minimum[10] or width of minimum method is used. In this method

$$\text{VSWR} = \frac{\lambda}{\pi \Delta}$$

where Δ is the position width of minimum at the points where the probe pickup is twice the minimum value. Then

$$Q \approx \frac{\lambda}{\pi\left(|x| + \frac{1}{|x|}\right)\Delta_{\text{test}}}.$$

In practice, the measurement system losses are significant compared to the test component loss, particularly at the higher frequencies, and must be corrected for. The loss correction is determined from the open and short VSWR data. Because the loss is low it can be shown that

$$Q \approx \frac{\lambda}{\pi\left(|x| + \frac{1}{|x|}\right)(\Delta_{\text{test}} - \Delta_{\text{correction}})}. \quad (7)$$

Both Δs must be corrected to the same point on the slotted line. The output reference plane of the line is used.

Several sources of error in the Q measurement are discussed in the Appendix. More will be said about the effects of these inaccuracies when specific results are given. However, an examination of (7) reveals the general behavior of the errors. Since λ is inversely proportional to frequency, the Δ difference in the denominator decreases sharply with frequency. The uncertainties in the measurement of Δ (see Appendix) thus contribute increasing percentage error with increasing frequency. Consequently, the determinations are accurate at 0.5 GHz but deteriorate with increasing frequency.

IV. Inductor Results

A variety of inductors has been built and tested. Circular spirals have been used in preference to square spirals as tuning elements in an effort to achieve improved Q. These coils were designed using low-frequency inductor formulas.[11],[12] Equation (8) has been found to be in fairly good agreement with experimental results. Errors of about 20 percent have been measured. The formula is[11]

$$L = \frac{a^2 n^2}{8a + 11c} \quad (8)$$

where

$a = (r_o + r_i)/2$
$c = r_o - r_i$
r_i is the inner radius of the spiral in mils
r_o is the outer radius of the spiral in mils
L is the inductance of the spiral in nanohenries
n is the number of turns.

Square spirals have been designed[13] and fabricated as chokes as described in Section VI.

The fabrication of thick spiral inductors with a cross section similar to that shown in Fig. 1(a) has been difficult in the past[14],[15] principally because of problems connected with making a satisfactory photoresist plating form. We have achieved such coils by plating copper into a thick Shipley-photoresist form.[3] Coils up to 1 mil thick have been made in this way. The dc resistance of these coils has been about $1\frac{3}{4}$ times the value expected for pure copper. The substrate material has been either glass or Al_2O_3. Silicon dioxide is used to insulate the crossovers in integrated circuit applications of these inductors.

A photograph of a 25 nH copper coil is shown in Fig. 4. The coil conductor is 2.5 mils wide and 0.5 mil thick with a 1.5 mil spacing between turns. This coil was tested by the methods described previously. A plot of Q^2 versus f for this coil is shown in Fig. 5. The Q increases as the square root of frequency, as expected from the considerations described earlier. Assuming bulk resistivity, the measured Q is approximately one half of that to be expected if the current

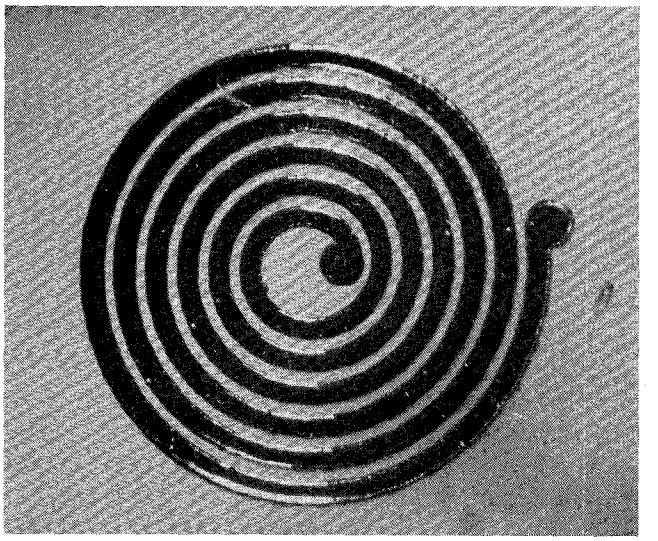

Fig. 4. Photograph of 25 nH inductor.

[3] For processing instructions see Shipley Company, Inc. bulletins.

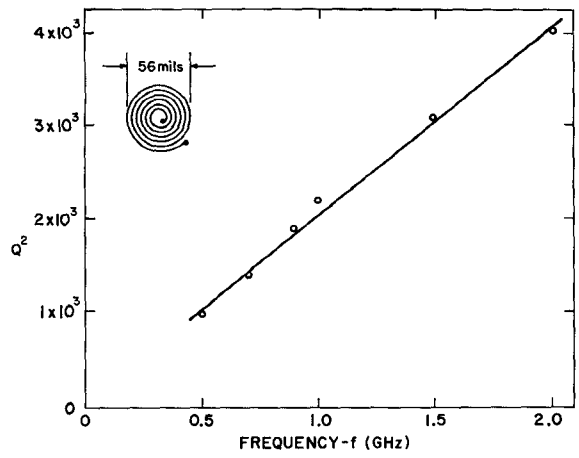

Fig. 5. Measured frequency variation of inductor Q for the Fig. 4 coil.

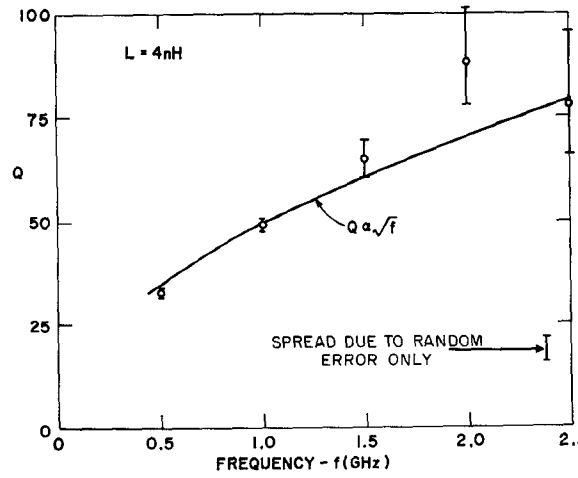

Fig. 6. Measured frequency variation of inductor Q for a 4 nH coil.

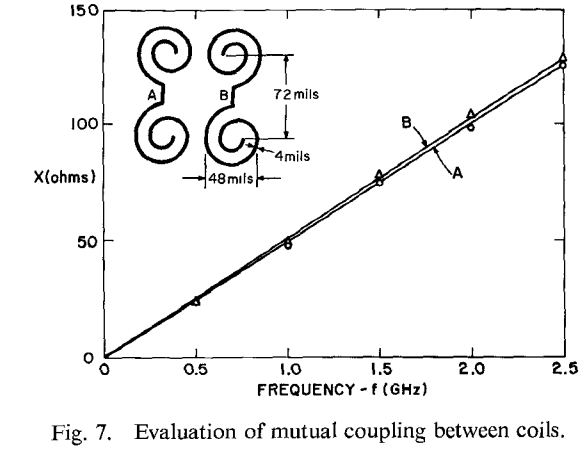

Fig. 7. Evaluation of mutual coupling between coils.

divided itself equally between the upper and lower surfaces of the coil. The accuracy of this Q measurement is enhanced by the fact that the 25 nH coil yields a relatively large reactance over the entire frequency band of the measurement.

Four nanohenry copper coils, a size more suitable for matching circuits at 2 GHz, were tested. The coil conductor is 4 mils wide and 10 microns thick. The coil has $1\frac{3}{4}$ turns with an outside diameter of 48 mils. Fig. 6 shows the measured frequency variation of inductor Q for this coil. The curve shows a Q is proportional to $\sqrt{f}$ variation. The open correction for line loss was used in the measurement of this coil. Although this leads to a conservative result relative to the use of the short correction, the Q values given in Fig. 6 may be somewhat optimistic at the upper edge of the frequency band, as explained in the Appendix. There is no correction for lead loss or connecting joint loss in the results given. The possible uncertainty in the Q values due to random error in the measurement of the Δ s is shown in Fig. 6.

The accuracy of the Q measurements, though limited, is good enough to permit the following two conclusions:

1) The inductor Q increases with frequency; the rate of increase approximates the expected square root of frequency dependency.
2) Q s greater than 50 are at present attainable for such coils in the lower S-band region. With improved conductivity and optimized coil design, Q s of 100 at these frequencies are a distinct possibility.

The dependency of Q on thickness was determined for a multiturn coil similar to the 25 nH coil of Fig. 4. Varying the thickness from 10 microns to 4 mils produced essentially no change in the Q. It is concluded then that two or three skin depths is the upper useful thickness for such a coil. The dependency of Q on conductor width has not yet been evaluated.

Fig. 7 is a plot of reactance versus frequency for a series connection of two of the Fig. 6 coils. Series connection A is electrically identical to series connection B except for the effect of mutual coupling between the coils. The plot shows that the mutual effect is negligible in this case. The smooth variation of X with frequency demonstrates the reliability of the reactance measurements, the coil behaves as a simple lumped element inductor.

V. Capacitor Results

The thin-film capacitor is the most desirable type for microwave integrated circuits. Thin-film capacitors have been constructed using deposited SiO_2 as a dielectric. The deposition technique is the controlled oxidation of silane.[16] Capacitors ranging from 1.5 to 50 pF have been built on glass or Al_2O_3 substrates. These capacitors have a dielectric layer 1 micron thick and range in size from 7 to 44 mils on a side. Measured Q values have clustered around the 40 to 60 level and were essentially constant across the band 0.5 to 2.5 GHz. It has been shown in an earlier section that capacitor Qs of several hundred should be possible if dielectric films having properties close to pure SiO_2 can be produced. The quality of the dielectric obtained from the present deposition technique can be improved, and indeed Texas Instruments Incorporated has reported[17] Q s of 100 at 2 GHz for thin-film capacitors containing reactively sputtered SiO_2.

VI. Lumped Element Power Amplifiers

Thin-film inductors and capacitors have been utilized in several single-stage 2 GHz transistor power amplifiers. Lumped element circuits were designed to match to 50 ohms the measured dynamic input and output impedances of an experimental RCA transistor pellet operated in a common-base class C mode.

The design of these transistor power amplifiers involves two steps: a) the determination of the transistor's input and output dynamic impedances, and b) the design of matching networks which can be realized with thin-film lumped elements.

The first step is accomplished by mounting the transistor chip on a calibrated microstrip test fixture which is attached to a coaxial measurement system.[18] The transistor is tuned for maximum power gain. The external tuning circuits are removed and their impedances measured using a slotted line to determine the optimum source and load impedances transferred to the connection plane of the transistor. It is important to keep the lengths of microstrip and coaxial lines to the tuners short, in order to reduce the effect of their attenuation on the accuracy of the measurements. This empirical method of transistor characterization was used rather than the linear approach found in small signal transistor circuit design[8] because no practical model for the nonlinear behavior of transistors operating in high-power class C amplifier circuits exists at present.

The input and output matching networks should have low loss and provide the optimum dynamic load and source impedances as measured at some specific operating condition. There should be a minimum number of elements in the matching networks in order to minimize losses. To achieve circuits of small size the area occupied by the matching networks should be comparable, within an order of magnitude, with the area of the transistor pellet. During the early work, bandwidth was not a constraint. In fact, designing for a narrow bandwidth would have caused intolerable losses since the particular transistors used have low-loaded Qs.

The requirements listed above can be met by using two-element L networks. This type of network can be easily designed using an impedance admittance chart.[19] A circuit so designed is shown in Fig. 8. Both the input and output impedances can be matched to 50 ohms by any of four different L networks. The choice of which network to use depends on losses, ease of bias connection, and whether the circuit is to be "breadboarded" or "integrated."[4] Assuming that each of the matching elements has a Q of 50 the total loss in the amplifier matching circuits varies from 0.5 to 1.0 dB depending on the configuration chosen. The loss of the circuit of Fig. 8 is 0.7 dB.

[4] As used here, the term breadboard refers to circuits constructed of separately mounted capacitors and inductors interconnected by ultrasonically bonded wires. The term integrated refers to a circuit with no bonds other than those necessary for the transistor connections.

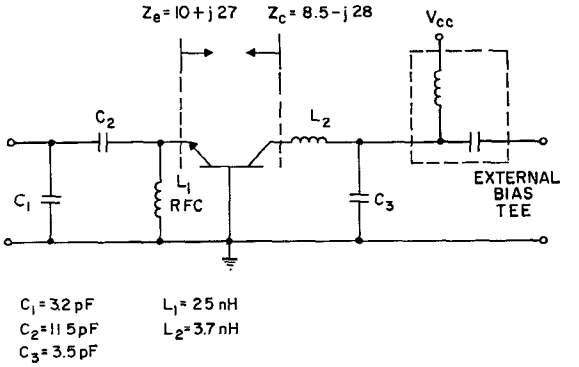

Fig. 8. Circuit diagram for lumped component power amplifier.

A. Breadboard Amplifier

Fig. 9 is a photograph of a breadboard form of the circuit depicted schematically in Fig. 8. Capacitor C_2 has little effect on the input match and is eliminated. OSSM flange mounts are used; they are beveled to facilitate connecting components. The proper values for C_1 and C_3 are achieved by connecting two capacitors in parallel. The circuit ground was brought out to the substrate edge and then silver painted over the edge to the grounded heat sink. The dark areas under the inductors are holes in the heat sink to minimize field distortion.

All interconnections were made by ultrasonically bonding with 1 mil diameter gold wire, which has an inductance of approximately $\frac{1}{4}$ nH per 10 mils of length. Since 1 nH at 2 GHz is 12.5 ohms, the lead lengths are important and must be carefully accounted for during layout. For this reason, several leads are paralleled where inductance is to be minimized.

Tests were made by externally tuning the amplifier for optimum performance, and then determining the impedances at the circuit connection points. In this manner, information was obtained from which the circuit components could be varied to achieve the desired performance.

After adjusting the output circuit elements, this amplifier had input–output matches of 1.5 to 1 and 1.9 to 1, respectively, at 2 GHz for a drive level of 19 dBm.

Fig. 10 is the gain frequency response of this amplifier with a constant drive level. At an input power level of 19 dBm, the 1 dB bandwidth was 9 percent, with a center frequency close to 2 GHz. The response characteristic varied considerably with drive level. This behavior is caused by the device's impedance variations with frequency and drive level. Fig. 11 shows the dynamic characteristics of the amplifier at 2 GHz. A maximum gain of 4.7 dB, with a collector efficiency of 9 percent, was obtained at an input drive of 50 mW. This gain did not occur (see Fig. 10) at the design drive level of 80 mW. However, the same chip when optimally tuned in a microstrip test fixture at the same drive and supply conditions exhibited a gain of 5.4 dB, 15 percent collector efficiency, and an output power of 350 mW. Obviously, the

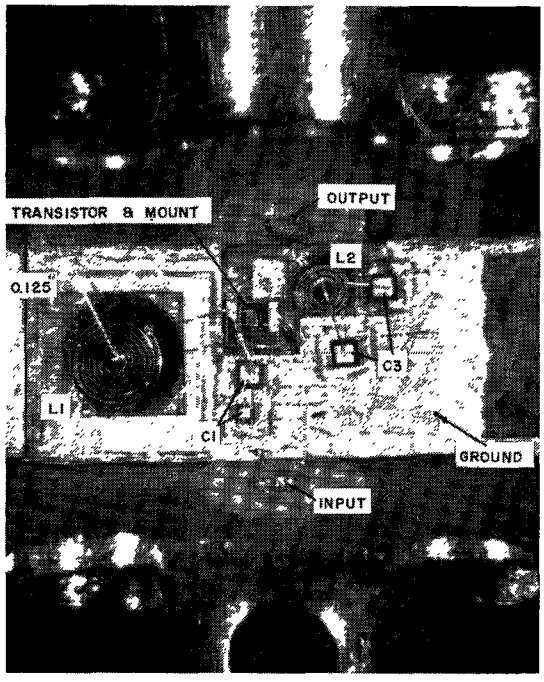

Fig. 9. Photograph of breadboarded lumped component power amplifier.

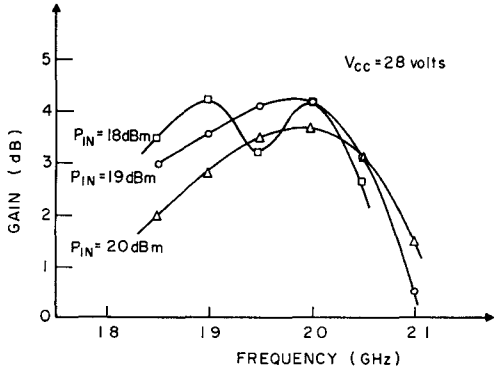

Fig. 10. Frequency response of Fig. 9 amplifier.

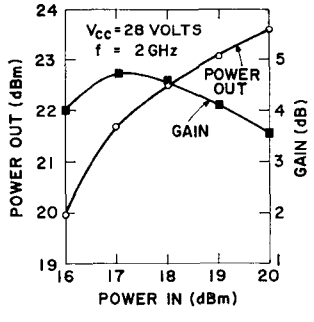

Fig. 11. Dynamic response of Fig. 9 amplifier.

amplifier was not optimally tuned and considerable degradation occurred due to the mismatches.

This particular batch of transistor chips exhibited an increase in collector efficiency and a decrease in gain when tuned at the higher drive level. Therefore, to improve the overall performance, an attempt was made to retune the amplifier. With a matched input and a 3 to 1 VSWR on the output, a gain of 3.6 dB, 17 percent collector efficiency, and 420 mW output power were achieved. The output was matched to 50 ohms by using an external stub tuner. These results are to be compared with the microstrip test fixture data of 3.7 dB gain, 23 percent collector efficiency, and 470 mW output.

Six breadboards have been built and tested to date. None has oscillated; all have performed in a similar fashion, i.e., optimum input and output matches have not been simultaneously achieved at a given drive level. Chips from another experimental run of transistors have yielded higher collector efficiencies, up to 27 percent, and higher output powers, even though their circuits were not optimized.

B. Integrated Amplifier

The breadboarding technique previously described has been useful in demonstrating the feasibility of lumped element microwave integrated circuits. However, the circuits described are a far cry from an integrated amplifier. This section describes briefly a preliminary integrated amplifier similar to that previously breadboarded. The circuit was changed to minimize area and the component interconnection lengths.

Fig. 12 is a photograph showing a portion of a 1 by $\frac{3}{4}$ inch sapphire substrate on which 45 thin-film 2 GHz power amplifier circuits were processed simultaneously. Each circuit contains all necessary elements required for biasing, stage isolation, and tuning. All components are thin-film lumped elements except for the transistor.

Fig. 13 is a detailed view of an individual amplifier and its circuit. In contrast to microstrip amplifiers, the transistor size is about equal to the other circuit elements. A 2 GHz microstrip amplifier using the same transistor and designed for minimum size is about ten times larger.

A desirable feature to design into integrated circuits is the ability to vary component values over a range sufficient to tune the device's expected impedances. This feature was incorporated to some extent in this layout; the top plate area of capacitors C_1, C_2 and C_4 can be increased by silver painting. However, the range available here is not sufficient and future designs must allow more area for this feature plus an additional variable capacitor in series with the inductors so that their values may also be changed.

The top ground area was centralized and is connected through the substrate to the lower ground plane by two "plated-through" holes. Results on the breadboard amplifiers have shown that silver painting the ground over the substrate edge is sufficient and is at present a more econom-

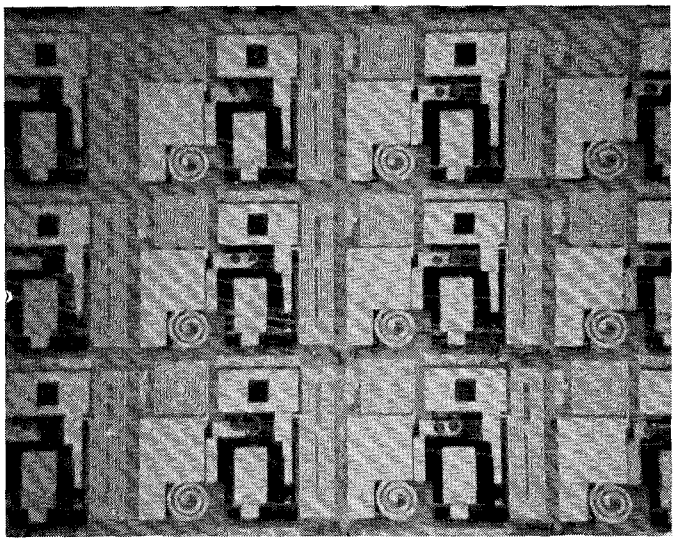

Fig. 12. Photograph of batch fabrication of amplifier circuits.

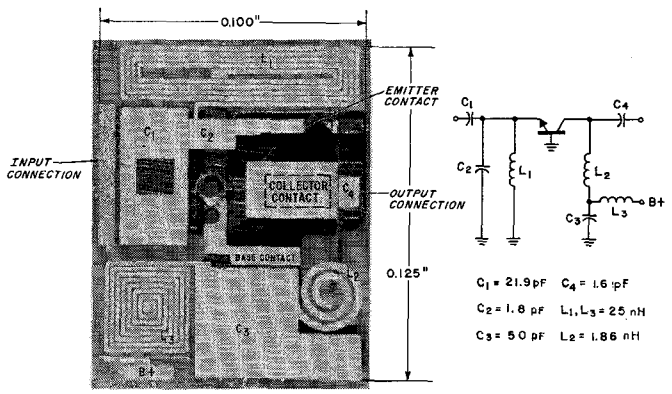

Fig. 13. Individual integrated amplifier and its circuit diagram.

ical technique. This latter technique will be used in future versions to increase yields.

The amplifier shown has not been tested at the time of this writing and is included only to show how lumped elements may be used in integrated amplifiers.

VII. Applications

The construction of microwave integrated circuits can be monolithic (active and passive devices grown into or on a semiconducting or active substrate), hybrid (passive elements deposited on a passive substrate and the active devices bonded and wired into place in a final step), or a quasi-monolithic combination of the two. The monolithic approach offers the possibility of processing more circuits with a minimum of handling, but the most suitable substrate, silicon, is lossy at microwave frequencies. If silicon is used as any part of a field carrying region, such as a support for inductors or an insulating dielectric for distributed elements, the Q will be severely degraded.

Lumped element circuits, with their small size, are very suitable for a quasi-monolithic approach similar to that described by the Decal Circuit Process.[20] Here the active elements can be grown into silicon, the lumped passive elements metalized around the active device, and the substrate then covered and fastened with glass. Finally, the lossy silicon can now be removed from the field carrying regions, and the circuit, which was quasi-monolithically grown, is now dielectrically isolated. The use of lumped elements makes this approach compete with distributed element hybrid circuits.

Lumped elements, mainly because of their small size (low Q), will not find application in critical narrowband high-efficiency amplifier stages, but they can be used in wideband, low- or medium-power stages. Here the amount of power lost in the elements will not be excessive. We envisage high-gain low-power cascaded S-band amplifiers which are quasi-monolithically constructed of lumped element circuits within a small area of perhaps 0.25 inch square. This small package can be fastened to the input of a final high-power higher Q microstrip hybrid amplifier.

Lumped elements can also be used as adjuncts to distributed circuits. One example is lumped element RF chokes which can save much space. Another example is lumped capacitors in series with microstrip lines. Since distributed tuning elements are mainly of a shunt nature, a lumped series high-Q capacitor could simplify networks of microstrip distributed elements.

VIII. Conclusion

Lumped elements suitable for use up to 2.5 GHz have been constructed. The elements have been evaluated using a simple impedance method which gives reasonable accuracies for the frequency range from 0.5 to 2.5 GHz. Both inductors and capacitors have exhibited Qs greater than 50 at lower S band. Simple transistor amplifier circuits have been wired together using lumped elements. Gains up to 4.7 dB were achieved at 2 GHz. The lumped element matching networks had a loss of about 0.5 dB greater than the loss in the distributed matching networks used in a microstrip amplifier built with the same type transistor. It is expected that the lumped circuit loss can be diminished as improved components are developed. Thus, the feasibility of lumped element microwave integrated circuits is demonstrated.

We conclude that because of their size and cost advantage lumped microwave integrated circuits will compete with distributed circuits in many applications at the lower microwave frequencies.

Appendix

Q Error

There are several sources of error in the Q measurement: mismatch error, correction error due to phase differences between the test and correction cases, and random error in the measurement of Δ.

The impedance measurement method assumes that the transmission line is perfectly matched between the slotted

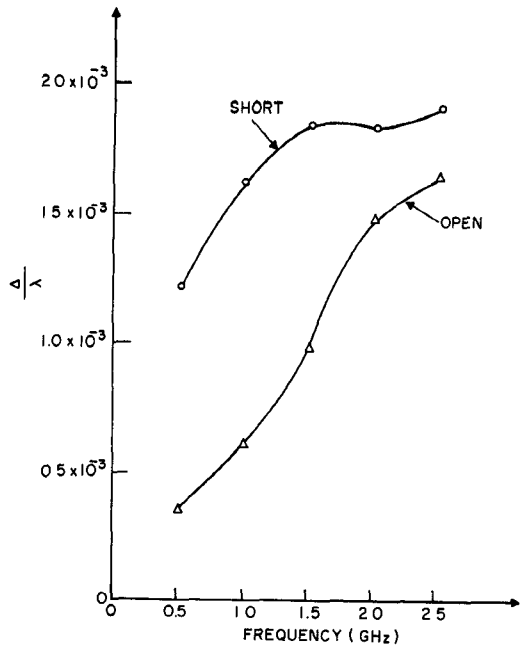

Fig. 14. Comparison of measurement system loss corrections.

line probe and the component mounting terminal. Actually, the transition from coaxial to microstrip lines introduces a small mismatch; in the frequency range of interest this mismatch causes a VSWR up to 1.05. Assuming that the mismatch impedance is reactive, this mismatch will cause an error of about ± 5 percent in the Q value. Since the discontinuity impedance is likely to be a parallel capacitance, the measured Q of an inductor is likely to be lower than the real Q.

The measurement system losses are conductor losses. Because the transverse dimension of the transmission line is much smaller in the test fixture than in the slotted line, the resistance per unit length is much larger in the test fixture. Consequently the measurement system losses depend on the phase of the current standing wave along the line. Fig. 14 is a comparison of measurement system loss with the fixture terminated in a short and in an open. Assuming low loss, it can be shown that the measurement system power loss divided by the incident power is proportional to Δ/λ. The short losses are greater because of the higher current concentration in the fixture in this case. The proper loss correction depends on the reactance of the test component. That is, the open correction is best applied to test components which have large reactances, and the short correction to those having small reactances. At 0.5 GHz, the short and open corrections are upper and lower bounds on the proper correction. However at 2.5 GHz, because the high-loss region covers an important percentage of the $\lambda/4$ phase variation, the proper correction can fall outside of this range. The uncertainty in the correction at the higher frequencies can result in optimistic inductor Qs. A more accurate correction can be determined by experimentally evaluating the measurement system loss as a function of phase for each frequency.

Finally there is a random error of about ± 0.015 mm in the measurement of the Δs. We take as a conservative estimate that the possible error in the difference of two such measurements is therefore ± 0.03 mm.

Acknowledgment

The authors wish to acknowledge the aid of the many people in the Microwave Research Laboratory who contributed to this work. The competent assistance of R. E. Chamberlain, R. D. DiStefano, N. Klein, and A. F. Young in constructing these elements is appreciated. The advice, criticism, and discussions with Drs. H. Sobol, L. S. Nergaard, and L. S. Napoli is gratefully acknowledged. Dr. H. Johnson of RCA Laboratories has been a strong proponent of the use of lumped elements at microwave frequencies, and the results reported herein are, in part, a tribute to his foresight.

References

[1] A. Ertel, "A 9 GHz silicon monolithic integrated TR switching circuit," Internat'l Electron Devices Meeting, October 1966.

[2] T. E. Saunders and P. D. Stark, "An integrated 4 GHz balanced transistor amplifier," Internat'l Solid-State Circuits Conf., February 1966.

[3] C. Genzabella and C. Howell, "Integrated *S*-band mixers," *IEEE Internat'l Conv. Rec.*, pt. 5, p. 113–118, March 1966.

[4] R. R. Webster, "Integrated microwave oscillators, amplifiers, switches, and converters," Internat'l Solid-State Circuits Conf., February 1967.

[5] A. Uhlir, Jr., "Microwave applications of integrated-circuit techniques," *Proc. IEEE*, vol. 52, pp. 1617–1623, December 1964.

[6] B. T. Vincent, Jr., "Microwave transistor amplifier design," presented at the Microwave Theory and Techniques Symp., May 1965.

[7] H. Johnson, RCA Lab., Princeton, N. J., November 1965 (private communication).

[8] R. W. Wyndrum, Jr., "The design of thin-film lumped element UHF amplifiers," Proc. Nat'l Security Industrial Association/Air Force Systems Command Microelectronics Conf., Washington, D. C., December 1965.

[9] S. Ramo, J. R. Whinnery, and T. Van Duzer, *Fields and Waves in Communication Electronics*. New York: Wiley, 1965, pp. 39–43 and pp. 330–334.

[10] E. L. Ginzton, *Microwave Measurements*. New York: McGraw-Hill, 1957, p. 266.

[11] F. E. Terman, *Radio Engineers Handbook*. New York: McGraw-Hill, 1943, p. 47.

[12] F. W. Grover, *Inductance Calculations*. Princeton, N. J.: Van Nostrand, 1946.

[13] H. G. Dill, "Designing inductors for thin-film applications," *Electronic Design*, pp. 52–59, February 17, 1964.

[14] F. R. Gleason, "Final development report for miniature thin-film inductors," Integrated Electronics Research Dept., Motorola, Inc., Scottsdale, Ariz., in contract with Navy Dept. Bureau of Ships, Contract NObsr 85397, Index SR-00803, Task 9636, June 30, 1964.

[15] A. E. Mason, Jr., "Study of solid-state integrated microwave circuits," Sci. Rept. 1, U4-811500-4, Texas Instruments Inc., in contract with NASA, Cambridge, Mass., Contract NAS 12-75, Control ERC/R&D 65-45, December 31, 1965.

[16] N. Goldsmith and W. Kern, "The deposition of vitreous silicon dioxide films from silane," *RCA Rev.*, vol. 28, pp. 153–165, March 1967.

[17] "Molecular electronics for radar applications," 3rd Interim Rept., Phase 2, Texas Instruments Inc., Rept. TI-03-66-80, Contract AF 33(615)-2525, DDC Rept. AD-484 739, June 1966 (unclassified).

[18] H. C. Lee, "Microwave power generation using overlay transistors," *RCA Rev.*, pp. 199–215, June 1966.

[19] J. G. Linvill and J. F. Gibbons, *Transistors and Active Circuits*. New York: McGraw-Hill, 1961.

[20] A. I. Stoller, J. A. Amick, and N. E. Wolff, "Getting the most out of circuits with dielectric isolation," *Electronics*, pp. 97–105, March 20, 1967.